Ceramics International 47 (2021) 30974–30979

Contents lists available at ScienceDirect

Ceramics International

journal homepage: www.elsevier.com/locate/ceramint

Cracking in the translucent alumina ceramic during flame thermal shock

Yuqiao Li [a,c], Qingxian Li [a,c], Xiaofeng Wu [b], Yingfeng Shao [a,c,*], Long Li [a,c,**], Fan Song [a,c]

[a] State Key Laboratory of Nonlinear Mechanics and Beijing Key Laboratory of Engineered Construction and Mechanobiology, Institute of Mechanics, Chinese Academy of Sciences, Beijing, 100190, China
[b] Beijing Institute of Structure and Environment Engineering, Beijing, 100076, China
[c] School of Engineering Science, University of Chinese Academy of Sciences, Beijing, 100049, China

ARTICLE INFO

Keywords:
Thermal shock
Cracking
Ceramic
Real-time
Crack speed

ABSTRACT

Crack measurement after thermal shock is usually considered as a replacement because real-time observation of thermal shock experiments is difficult to achieve. This paper presents an experimental approach for real-time displaying thermal shock cracking using oxygen-acetylene flame and high-speed imaging of translucent ceramic. We capture the crack propagation process, calculate the crack propagation speed, discuss the effect of sample size and flame heat flux on the crack propagation, and analyze the difference between the crack propagation under cold shock and hot shock. This paper further improves the mechanism of thermal shock damage of ceramic materials.

1. Introduction

The chemical and mechanical stability at high temperatures makes ceramic materials widely used in high-temperature industrial environments, especially in the aerospace field [1–4]. Ceramics serving in high-temperature environments usually undergo rapid heating and cooling processes, leading to large thermal stresses [1,2]. Due to inherent brittleness, severe thermal shock conditions can lead to microstructure damage or catastrophic failure of ceramic [3,4]. Therefore, thermal shock resistance has become one of the critical criteria for selecting and designing ceramics.

The thermal shock test of material can be divided into two types: cold shock and hot shock. The former is usually tested by the water quenching method that the sample is heated to a specific temperature and then thrown into the cold shock medium [5,6]. Hot shock generally adopts the technique of rapidly heating the specimen, such as laser [7], flame [8], irradiation [9], arc wind tunnel heating [10], etc., for testing. The material's cold and hot shock resistance is evaluated by observing the crack morphology and measuring the residual strength of the specimen [5–10]. With the in-depth study of thermal shock damage mechanism, it is becoming more critical to confirm the occurrence and development process of the thermal shock. Consequently, there is an urgent need for methods to observe the complete process of the thermal shock.

As to the real-time observation of the cold shock cracking process, we have realized it through the water quenching process of the translucent material in the early stage [11]. However, there are few real-time observations of the hot shock cracking process, and most of the previous experiments are mainly crack measurements after hot shock [1,9]. The possible difficulty is how to avoid the influence of the hot shock process on the capture of rapid crack growth. In this paper, we use a particular device for the hot shock of translucent ceramic sheets. A high-speed camera is applied to capture hot shock cracking in real-time and calculate the crack propagation speed. Besides, we compared the results with that of crack propagation under cold shock.

2. Experimental procedure

2.1. Flame hot shock test

Translucent alumina was made from 0.8 μm Al_2O_3 powder (99.4%, Jiawei Ceramics Co., Ltd., Zhuhai, China) by tape casting, calcining in the air at 800 °C and sintering in the hydrogen at 1700 °C for 2 h. The average grain size and the ceramic density were 20.8 μm and 3.95 g/

* Corresponding author. State Key Laboratory of Nonlinear Mechanics and Beijing Key Laboratory of Engineered Construction and Mechanobiology, Institute of Mechanics, Chinese Academy of Sciences, Beijing, 100190, China.
** Corresponding author. State Key Laboratory of Nonlinear Mechanics and Beijing Key Laboratory of Engineered Construction and Mechanobiology, Institute of Mechanics, Chinese Academy of Sciences, Beijing, 100190, China.
E-mail addresses: shaoyf@lnm.imech.ac.cn (Y. Shao), lilong@lnm.imech.ac.cn (L. Li).

https://doi.org/10.1016/j.ceramint.2021.07.154
Received 5 June 2021; Received in revised form 12 July 2021; Accepted 15 July 2021
Available online 16 July 2021

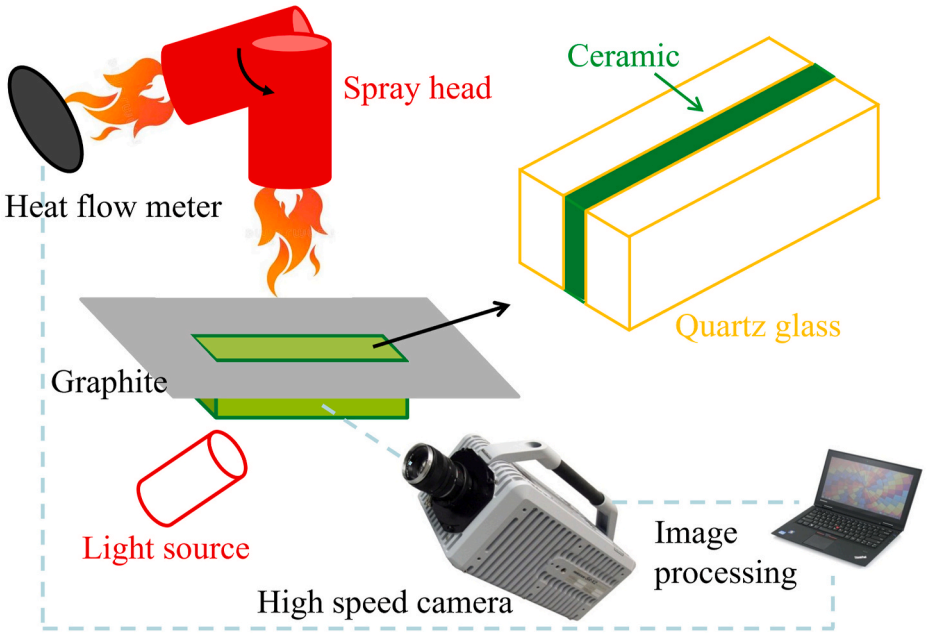

Fig. 1. Schematic of observation device of the ceramic cracking during flame hot shock.

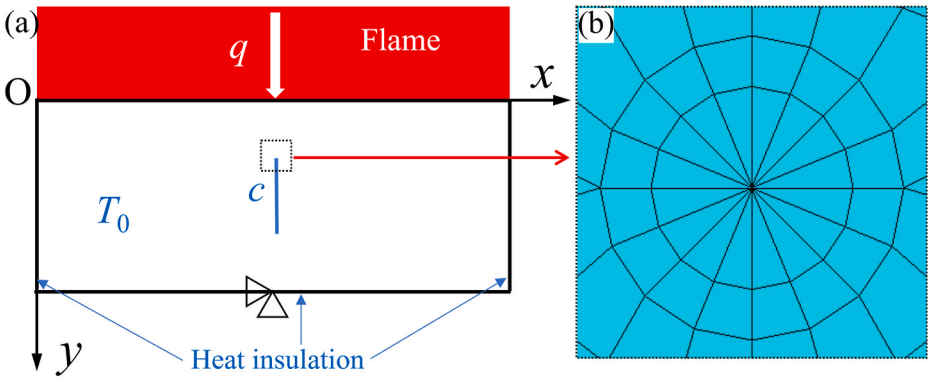

Fig. 2. (a) Finite element model for calculating the stress intensity factor at both ends of the central crack during hot shock (q is the flame heat flux, c is the central crack's length), (b) Finite element grid at the crack tip.

cm^3, which were measured by the line intercept method and the drainage method separately. The crack morphology during the oxyacetylene flame test was studied using ceramic sheets of 0.5 mm × 10 mm × 50 mm and 0.5 mm × 20 mm × 50 mm. To make only one side (0.4 mm × 50 mm) was heated by the flame, the ceramic sheet was placed between two quartz glass to assemble a sandwich structure, and a graphite plate with rectangular holes was employed to block the flame during the test. The above design restricts the flame to the target surface (0.4 mm × 50 mm) without affecting the side observation (10 mm × 50 mm or 20 mm × 50 mm), as shown in Fig. 1. This device also allows the sample to be heated more uniformly in the case of a large flame.

Place the sample on the focused workbench. In front of it, the flame nozzle was ignited and calibrated with a heat flow meter. We adjusted the flow of oxygen and acetylene to obtain the heat flux value required for the test. After that, we aligned the flame with the sample for testing. In the meantime, the high-speed camera (Phantom V2012, Wayne, NJ, USA) captured the image at a speed of 651,000 frames/s and a resolution of 128 × 64 pixels during the hot shock (The picture is small that it may not be precise enough), as shown in Fig. 1. By this means, crack initiation and propagation during hot shock can be successfully observed using the light refraction and reflection at the crack interface. The crack propagation speed can also be obtained by the crack length vs. time from a series of images recorded in the experiment.

Table 1
Mechanical and thermal parameters of alumina used in calculation.

Young modulus E (GPa)	Poisson's ratio ν	Heat flux q (MW/m^2)	Thermal conductivity k (W m^{-1} K^{-1})	Coefficient of thermal expansion α (10^{-6} K^{-1})	Specific heat c (J/kg K)
370	0.22	1.5	20	6.8	880

2.2. Finite element model for calculating stress intensity factor

Rapid heating of the surface creates instantaneous tensile stresses in the interior of the sheet. Therefore, the sheet is most likely to form mode I crack at the position where the maximum tensile stress is reached [12]. To compare crack propagation speed qualitatively, we calculate the stress intensity factors $\zeta i = \zeta 0\text{-}\ln\omega i 1/mK_I$ and K_I'' at the two ends of the pre-existing central crack c in a 10 mm × 50 mm ceramic sheet. We use a 2D plane stress finite element model with an element size of 0.05 mm. The crack tip singular element is transformed from the traditional quadrilateral element, which is realized by moving the middle node to a

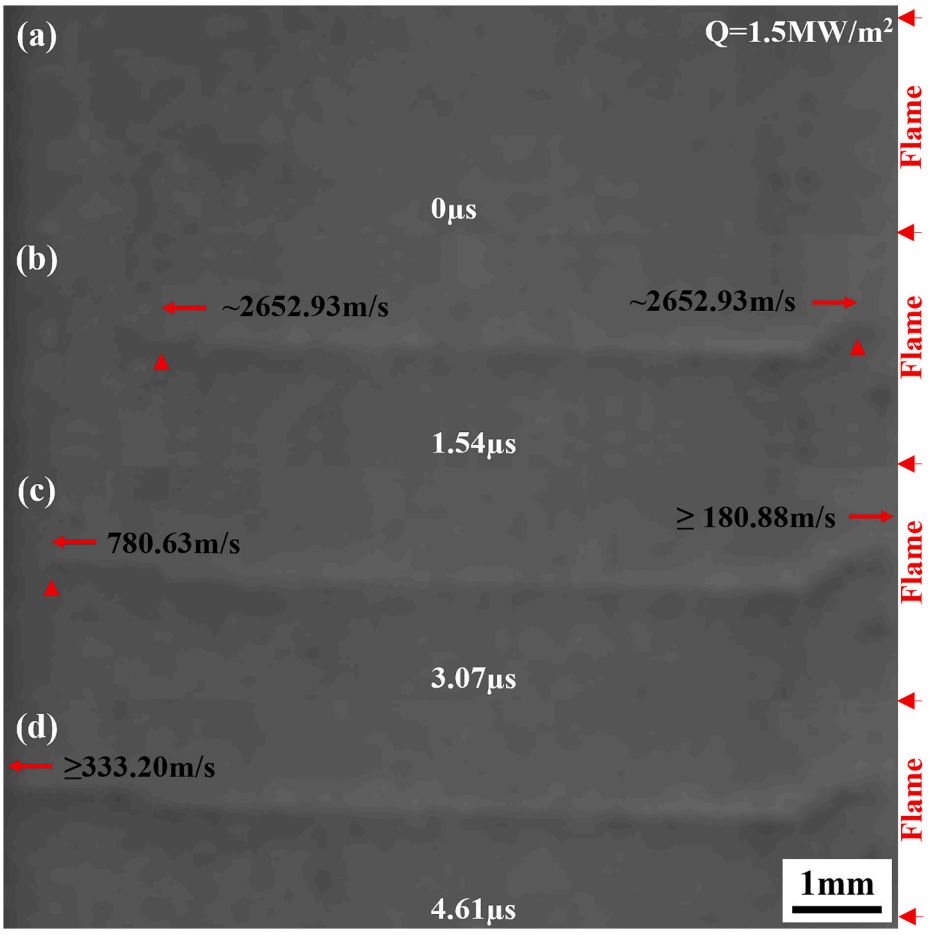

Fig. 3. (a)–(d) Images of crack initiation and propagation in 10 mm wide ceramic under flame hot shock of 1.5 MW/m^2 heat flux.

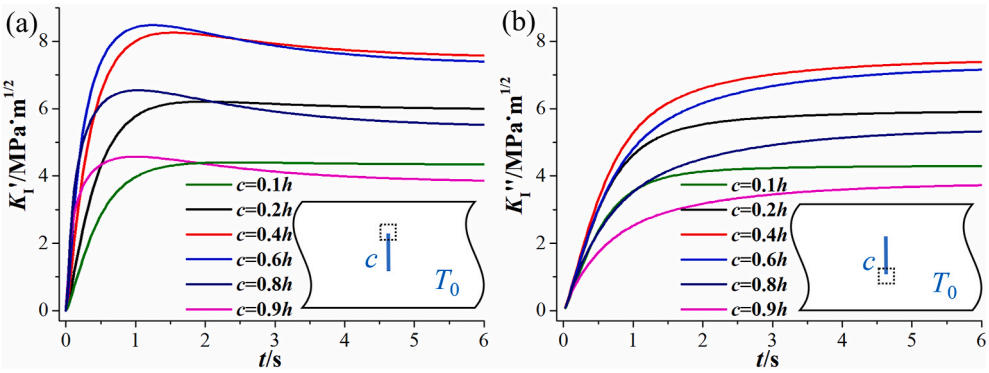

Fig. 4. Transient thermal stress intensity factors (a) K_I' and (b) K_I'' changing with time of 10 mm wide ceramic.

quarter. The representative grid and boundary conditions are shown in Fig. 2. The calculation parameters of alumina are shown in Table 1 [13].

3. Results and discussion

Fig. 3a–d shows the images of crack initiation and propagation in 10 mm wide ceramic under a flame hot shock of 1.5 MW/m^2 heat flux. We can see that the crack propagates very quickly, and the entire propagation process will be completed in 3 frames, about 5 μs The propagation process can be roughly divided into two stages. In the first stage, cracks suddenly appeared inside the sample within one frame at about 4 s after the flame spraying on the sample's surface. The average speed of propagation is about 2653 m/s, as shown in Fig. 3a. The cracks that appear in the materials are caused by the thermal stress exceeding the material's strength. In the second stage, the crack continues to propagate towards the boundary with significantly reduced speed. The sample will be broken entirely by forming a through crack in about 3 frames, as shown in Fig. 3. We can see that as the crack size increases, the stress intensity factors at the crack tips first increase and then decrease in Fig. 4. It may explain the phenomenon that the crack speed is fast at the beginning and then slows down.

Fig. 5a–d shows the images of crack initiation and propagation in 10 mm wide ceramic under a flame hot shock of 2.2 MW/m^2 heat flux. The crack propagation process is different from Fig. 3. In the first stage, a type-I crack suddenly appears inside the ceramic at about 3 s, and two ends of this crack branched to form 4 cracks after the crack propagates to

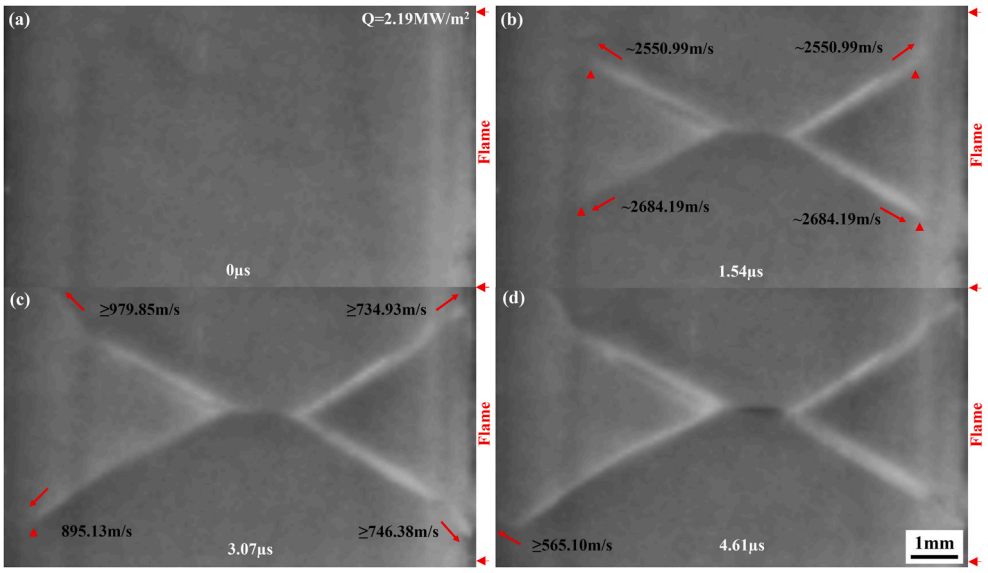

Fig. 5. (a)–(d) Images of crack initiation and propagation in 10 mm wide ceramic under flame hot shock of 2.2 MW/m^2 heat flux.

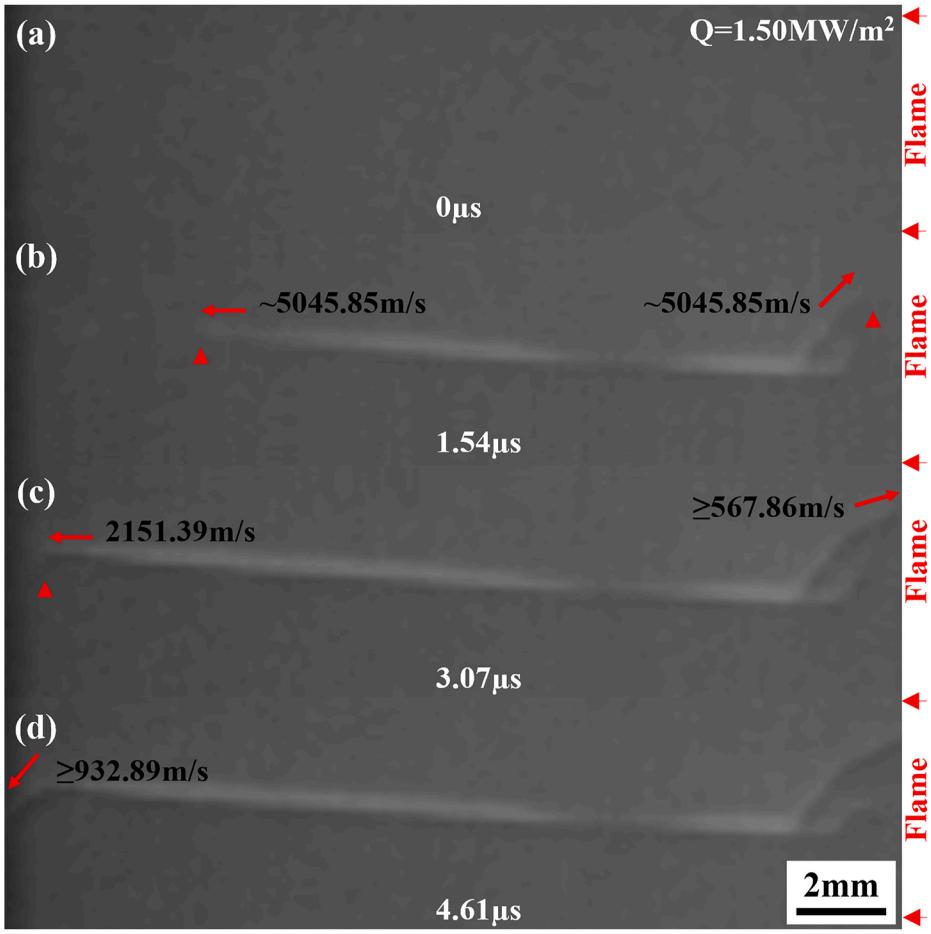

Fig. 6. (a)–(d) Images of crack initiation and propagation in 20 mm wide ceramic under flame hot shock of 1.5 MW/m^2 heat flux.

a certain length, as shown in Fig. 5b. We can see that there is an unstable crack bifurcation at the tip of the crack. It may be because of the higher instantaneous thermal strain energy of ceramics caused by the flame hot shock with higher heat flux leading to the cracks that move too fast to maintain stability [14]. To release excess energy, a complex fracture model appears in the sample. In the second stage, the bifurcation cracks continue to spread towards the boundary with significantly reduced speed until a through crack is formed in the sample.

Fig. 6a–d shows the images of crack initiation and propagation in a 20 mm wide ceramic under a flame hot shock of 1.5 MW/m^2 heat flux. Like

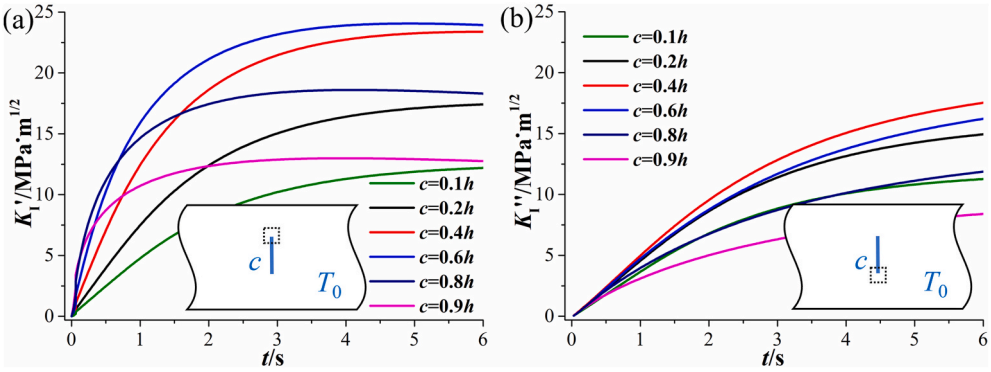

Fig. 7. Transient thermal stress intensity factors (a) K_I' and (b) K_I'' changing with time of 20 mm wide ceramic.

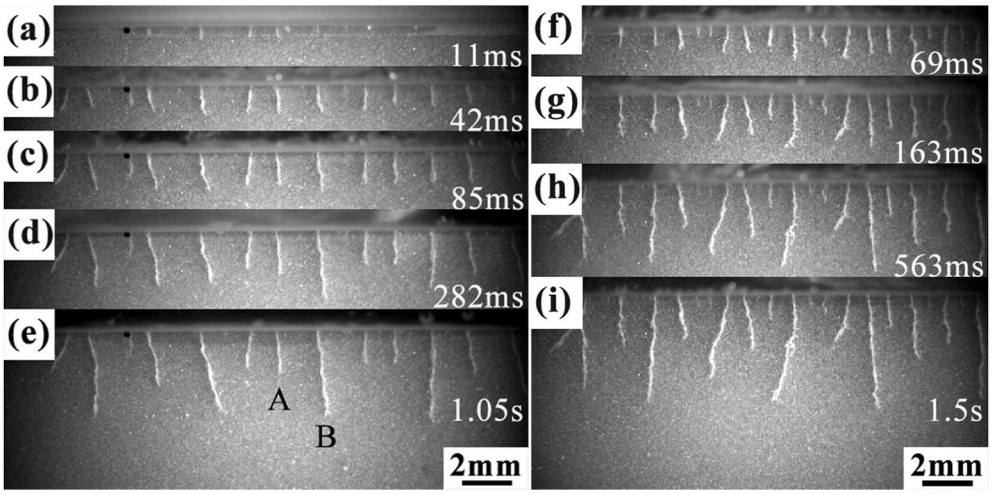

Fig. 8. Images of crack initiation and propagation in ceramics under quenching cold shock at temperature difference of (a)–(e) 280 °C; and (f)–(i) 430 °C.

the 10 mm wide specimen, cracks appear inside the sample within a certain frame in the first stage. However, the average crack propagation speed in the 20 mm specimen is about 4500 m/s which is faster than that of the 10 mm specimen. Unstable crack bifurcation has also appeared at the crack's tip, as shown in Fig. 6b. To qualitatively determine the effect of specimen size on crack propagation speed, we also calculated the transient thermal stress intensity factors of 20 mm wide ceramic, as shown in Fig. 7. Comparing with the result of 10 mm wide ceramic, we can see that when the time is greater than 1 s, the transient thermal stress intensity factors of both ends of the crack *c* of the 20 mm specimen are larger than those of the 10 mm specimen respectively. The larger the stress intensity factor is, the faster the crack propagation is and the easier the unstable propagation is. We can conclude that the larger the sample becomes, the faster and more unstable the crack will propagate. Besides, the bifurcated crack will continue to propagate at a slower speed.

Previously, we investigated the crack initiation and propagation on the ceramic sheet under water quenching by experiment and simulation [11,13]. We find that the cracks generate from the surface subjected to cold shock and propagate into the ceramic sheet (Fig. 8). Then, cracks propagate at intervals and form a hierarchical crack pattern [11,13], which is very different from a single internal crack under hot shock. This distinction is the disparate stress responses caused by the temperature fields inside the ceramics. The maximum tensile stress is generated on the ceramic sheet's surface during cold shock while inside during hot shock. Besides, there is a big difference in crack propagation speed. In cold shock, crack propagation can be regarded as a quasi-static process because its speed is less than 1 m/s. However, this speed may reach 4.5 km/s under hot shock, close to alumina's Rayleigh wave speed (6 km/s [15]). The difference should be due to the different strain energy release rates at the crack tip caused by the temperature field states of the ceramic. The above research on the crack speed of hot shock should be verification on the thermal shock models and simulations proposed by some scholars [16–19].

What's more, hot shock will cause severer damage than cold shock. The time for hot shock damage is too short to stop, even if turning off the flame halfway. Nevertheless, the material will not be completely destroyed after stopping the cold shock. It further reveals that the cold shock and hot shock tests of materials are irreplaceable to some extent. The water quenching test is used as a compromise method for the thermal shock that cannot truly reflect the hot shock process though it is convenient.

4. Conclusions

We obtain a real-time observation of ceramic flame hot shock by specially designed equipment. The results show that crack that appears from the inside of the ceramic and propagates to both sides will eventually form a through crack and cause catastrophic failure. The hot shock crack propagation speed is fast initially, close to the Rayleigh wave velocity, and then gradually decreases. The increase of heat flux and sample size can result in unstable crack bifurcation in crack propagation. Besides, the rise in the sample size may also increase the initial propagation speed. It is very different from crack propagation under cold shock. Therefore, cold shock and hot shock tests are not

interchangeable to some extent.

Declaration of competing interest

The authors declare that they have no known competing financial interests or personal relationships that could have appeared to influence the work reported in this paper.

Acknowledgments

This work was sponsored by the Strategic Priority Research Program of the Chinese Academy of Sciences [grant number XDB22040102]; the National Natural Science Foundations of China [grant number 11802033]; and Youth Innovation Promotion Association CAS.

References

[1] Y.W. Wang, B. Xia, H.H. Su, H. Chen, X. Feng, Improving the thermal shock resistance of ceramics by crack arrest blocks, Sci. China Technol. Sci. 59 (2016) 913–919, https://doi.org/10.1007/s11431-015-5978-x.

[2] W.E. Pompe, Thermal shock behavior of ceramic materials-modeling and measurement, in: G.A. Schneider, G. Petzow (Eds.), Thermal Shock and Thermal Fatigue Behavior of Advanced Ceramics, vol. 241, Kluwer Academic Publ, Dordrecht, 1993, pp. 3–14.

[3] K.S. Lee, Z. Meng, I.C. Sihn, K. Choi, J.E. Lee, S. Bae, H.I. Lee, Spherical indentations on hafnium carbide- and silicon-carbide-coated carbon–carbon composites after thermal shock test in air, Ceram. Int. 46 (2020) 21233–21242, https://doi.org/10.1016/j.ceramint.2020.05.211.

[4] A.Z. Wang, P. Hu, B. Du, C. Fang, D.Y. Zhang, X.H. Zhang, Cracking behavior of ZrB_2-SiC-Graphite sharp leading edges during thermal shock, Ceram. Int. 44 (2018) 7694–7699, https://doi.org/10.1016/j.ceramint.2018.01.195.

[5] T. Yoshimoto, S. Ishihara, T. Goshima, A.J. McEvily, T. Ishizaki, An improved method for the determination of the maximum thermal stress induced during a quench test, Scripta Mater. 41 (1999) 553–559, https://doi.org/10.1016/S1359-6462(99)00185-2.

[6] D.Y. Li, W.G. Li, W.B. Zhang, D.N. Fang, Thermal shock resistance of ultra-high temperature ceramics including the effects of thermal environment and external constraints, Mater. Des. 37 (2012) 211–214, https://doi.org/10.1016/j.matdes.2011.12.047.

[7] C.Y. Jian, T. Hashida, H. Takahashi, M. Saito, Thermal shock and fatigue resistance evaluation of functionally graded coating for gas turbine blades by laser heating method, Compos. Eng. 5 (1995) 879–889, https://doi.org/10.1016/0961-9526(95)00041-K.

[8] S.R. Levine, E.J. Opila, M.C. Halbig, J.D. Kiser, M. Singh, J.A. Salem, Evaluation of ultra-high temperature ceramics for aeropropulsion use, J. Eur. Ceram. Soc. 22 (2002) 2757–2767, https://doi.org/10.1016/S0955-2219(02)00140-1.

[9] G.A. Schneider, G. Petzow, Thermal shock testing of ceramics—a new testing method, J. Am. Ceram. Soc. 74 (1991) 98–102, https://doi.org/10.1111/j.1151-2916.1991.tb07303.x.

[10] X.H. Zhang, P. Hu, J.C. Han, S.H. Meng, Ablation behavior of ZrB_2–SiC ultra high temperature ceramics under simulated atmospheric re-entry conditions, Compos. Sci. Technol. 68 (2008) 1718–1726, https://doi.org/10.1016/j.compscitech.2008.02.009.

[11] Y.F. Shao, F. Song, B.Y. Liu, W. Li, L. Li, C.P. Jiang, Observation of ceramic cracking during quenching, J. Am. Ceram. Soc. 100 (2017) 520–523, https://doi.org/10.1111/jace.14674.

[12] B.L. Wang, J. Li, Thermal stress and intensity release in ferroelectric materials by multiple cracking, Acta Mater. 53 (2005) 785–799, https://doi.org/10.1016/j.actamat.2004.10.031.

[13] Y.F. Shao, B.Y. Liu, X.H. Wang, L. Li, J.C. Wei, F. Song, Crack propagation speed in ceramic during quenching, J. Eur. Ceram. Soc. 38 (2018) 2879–2885, https://doi.org/10.1016/j.jeurceramsoc.2018.02.028.

[14] J. Fineberg, S.P. Gross, M. Marder, H.L. Swinney, Instability in dynamic fracture, Phys. Rev. Lett. 67 (1991) 457–460, https://doi.org/10.1103/PhysRevLett.67.457.

[15] P.D. Zavattieri, H.D. Espinosa, Grain level analysis of crack initiation and propagation in brittle materials, Acta Mater. 49 (2001) 4291–4311, https://doi.org/10.1016/S1359-6454(01)00292-0.

[16] D.Y. Chu, X. Li, Z.L. Liu, Study the dynamic crack path in brittle material under thermal shock loading by phase field modeling, Int. J. Fract. 208 (2017) 115–130, https://doi.org/10.1007/s10704-017-0220-4.

[17] Y.T. Wang, X.P. Zhou, M.M. Kou, An improved coupled thermo-mechanic bond-based peridynamic model for cracking behaviors in brittle solids subjected to thermal shocks, Eur. J. Mech. A Solids 73 (2019) 282–305, https://doi.org/10.1016/j.euromechsol.2018.09.007.

[18] T. Wang, X. Ye, Z.L. Liu, X.M. Liu, D.Y. Chu, Z. Zhuang, A phase-field model of thermo-elastic coupled brittle fracture with explicit time integration, Comput. Mech. 65 (2020) 1305–1321, https://doi.org/10.1007/s00466-020-01820-6.

[19] D.Y. Li, W.G. Li, R.Z. Wang, H.B. Kou, Simulation of the thermal shock behavior of ultra-high temperature ceramics with the consideration of temperature-dependent crack propagation criterion and interaction between thermal shock cracks evolution and thermal conduction, Eur. J. Mech. A Solids 72 (2018) 268–274, https://doi.org/10.1016/j.euromechsol.2018.05.016.